



Effect of Ion Implantation on Layer Inversion of Ni Silicided Poly-Si

P. S. Lee,^a K. L. Pey,^{b,z} D. Mangelinck,^c J. Ding,^a D. Z. Chi,^d T. Osipowicz,^e
J. Y. Dai,^c and L. Chan^f

^aDepartment of Materials Science, ^bDepartment of Electrical and Computer Engineering, ^dInstitute of Materials Science and Engineering, and ^eDepartment of Physics, National University of Singapore, Singapore 11967

^cL2MP-CNRS, Faculte de Saint-Jérôme-case 151, 13397 Marseille Cedex 20, France

^fChartered Semiconductor Manufacturing, Limited, Singapore 738496

The effect of ion implantation on the behavior and extent of layer inversion in Ni-silicided poly-Si was investigated. Two different implantation species, namely, BF_2^+ and N_2^+ , which affect the poly-Si grain growth were used. Retarded layer inversion was found with the ion-implanted poly-Si substrates. However, the formation of NiSi_2 takes place at 700°C , which is slightly lower than that on $\text{Si}(100)$. The easy nucleation of NiSi_2 on poly-Si is implicitly related to the morphology perturbation.

© 2002 The Electrochemical Society. [DOI: 10.1149/1.1494828] All rights reserved.

Manuscript received December 10, 2001. Available electronically July 12, 2002.

Salicide material has encountered various challenges as complementary metal oxide semiconductor (CMOS) device dimensions shrink. The difficulty in the phase transformation of TiSi_2 from C49 to C54 phase has resulted in an increase in sheet resistance of the poly-Si lines as the linewidths reduce. The problems related to the scaling of the widely used TiSi_2 have initiated much investigation on other silicides. Currently sub- $0.25\ \mu\text{m}$ devices have replaced TiSi_2 with CoSi_2 . Although CoSi_2 has shown competency because its sheet resistance is independent of linewidth, the high Si consumption and junction leakage due to spiking or other mechanisms are critical problems for the future submicrometer CMOS applications. Much attention has been given to the search for an optimum salicidation material. NiSi has been given worthy consideration due to its several attractive features, which include low silicidation temperature ($400\text{--}600^\circ\text{C}$), lower Si consumption than TiSi_2 and CoSi_2 , lesser film stress, and good bridging resistance since Ni is the dominant diffusing species. The initial study of NiSi as a replacement material for salicidation was reported by Morimoto *et al.*¹ Stable sheet resistance was achieved at $0.4\ \mu\text{m}$ poly-Si linewidths after a 600°C , 30 s anneal. Aggressive device scaling has prompted further study of Ni silicides on linewidths about $0.1\ \mu\text{m}$.²

The thermal stability of thin silicide films on Si is a major concern, since it limits the thermal budget allowable for further processing. The microstructure of silicide films may degrade by grooving and islanding under excessive heat-treatment. Recently, new merged devices, such as logic and dynamic random access memory (DRAM), logic and radio frequency (rf), DRAM and rf, and so on, are now in demand. In the merged devices, there are various thermal processes, *e.g.*, annealing of the capacitor dielectric in DRAM ($\sim 800^\circ\text{C}$) and activation of impurities in device junctions ($\sim 900^\circ\text{C}$ and above). If these processes are carried out after silicide formation, it is necessary to find the means to suppress degradation of the silicide during subsequent processing.³ The well-known problems of NiSi are the relatively low thermal stability including phase transformation to the high resistivity NiSi_2 phase and morphology degradation after high processing temperatures. Silicide stability is usually less robust on the polycrystalline Si (poly-Si). On poly-Si, inversion in the respective positions of the silicide and the poly-Si due to poly-Si grain growth was reported to start at temperatures as low as 550°C with Ni silicides.⁴ This work aims to investigate the effect of ion implantation in poly-Si on layer inversion of Ni silicides. Two kinds of implant species were employed, namely, BF_2^+ and N_2^+ .

Experimental

Poly-Si was deposited using the conventional low pressure chemical vapor deposition (LPCVD) onto $\text{Si}(100)$ blanket wafers with gate oxide of $60\ \text{\AA}$. On the blanket poly-Si wafers, ion implantation was carried out using BF_2^+ with a dose of $3 \times 10^{15}\ \text{cm}^{-2}$ at $30\ \text{keV}$, followed by postimplant annealing at 925°C for 30 s. N_2^+ implantation was done with a dosage of $6 \times 10^{14}\ \text{cm}^{-2}$ at $15\ \text{keV}$ on the blanket poly-Si wafers, followed by postimplant annealing at 950°C , 60 s. The undoped and doped poly-Si wafers were sputtered with Ni of about $30\ \text{nm}$ after a dilute HF clean. The effect of different dopants on layer inversion of Ni silicides was analyzed using Rutherford backscattering (RBS), scanning electron microscopy (SEM), X-ray transmission electron microscopy (XTEM), and sheet resistance measurements.

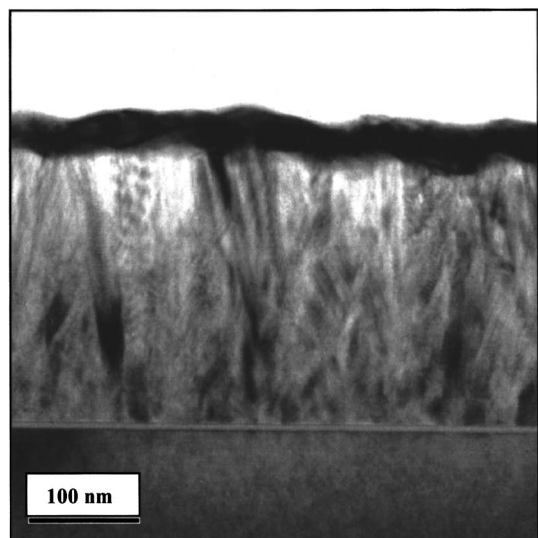
Results

Figures 1a and b show the XTEM micrographs of Ni on undoped poly-Si after annealing at 500 and 700°C . After silicidation at 500°C , NiSi forms on the poly-Si without any protrusions. The poly-Si grains still preserve the needle-like columnar form without obvious grain growth. It has been shown that without the silicide layer, poly-Si grains will not undergo significant grain growth up to 1000°C .⁵ With the presence of a silicide layer, which can act as a transport medium, layer inversion has occurred during which the Si grains underwent exaggerated grain growth (or secondary grain growth) and penetrate through the silicide layer to reach the free surface. The resultant topological inversion is shown in Fig. 1b. The poly-Si grains were large and relatively free of defects such as stacking faults that were present in the as-deposited Si layer (and even after 500°C silicidation as shown in Fig. 1a).

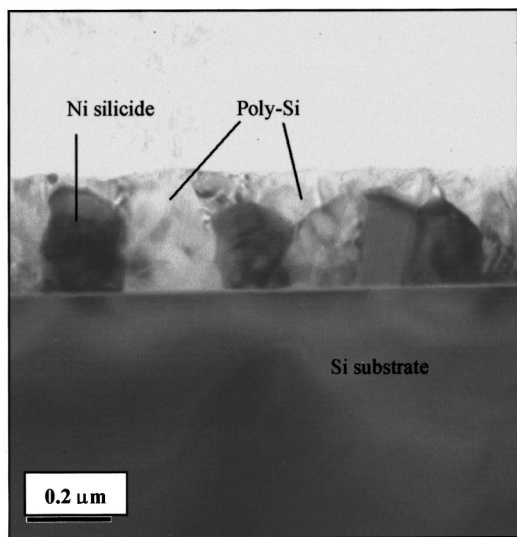
The progress of layer inversion was monitored using RBS analysis as shown in Fig. 2. At 500°C , the composition yield ratio corresponds to the formation of NiSi . After annealing at 600°C , the Ni yield experienced a sudden drop and the Si yield was relatively high and advanced to the surface. This is an indication of the occurrence of layer inversion. At 700°C , the Ni yield continues to lower and forms a broad bell shape. A similar spectrum was obtained at 900°C . This shows that the layer reconstruction begins at a low temperature of 600°C and continues even up to 900°C .

For samples with BF_2^+ implanted poly-Si with postimplant annealing, the RBS composition analysis was performed after silicidation at temperatures ranging from 500 to 750°C . As shown in Fig. 3, the composition yield corresponds to NiSi after 500°C anneal and remains unchanged after annealing at 600°C . This is in great contrast compared to the undoped poly-Si where layer reversal has started. Therefore, the suppression of layer inversion is clearly due

^z E-mail: elepeykl@nus.edu.sg



(a)



(b)

Figure 1. XTEM micrographs of Ni on undoped poly-Si after annealing at (a) 500 and (b) 700°C.

to the incorporation of dopants in the poly-Si layer prior to silicidation. At 700°C, a drop in yield occurs at the Ni peak, yet the peak is relatively symmetrical without much tailing affect. Simulation with RUMP suggests a composition ratio close to NiSi₂ at 700°C. After annealing at 750°C, the Ni peak shows a raising shoulder occurring at the bottom layer, and this corresponds to the intrusion of silicide, which is also reflected from the Si that extends to the free surface. Therefore, layer inversion is evident with the BF₂⁺ samples at 750°C, which is a relatively higher onset temperature compared to that on the undoped poly-Si.

Figure 4 shows the RBS spectra of Ni on N₂⁺ implanted poly-Si after annealing at various temperatures. The RBS composition ratio corresponds to NiSi at 500°C. After annealing at 700°C, the Ni yield falls and the ratio to Si is close to that of NiSi₂. At 750°C, tailing at the Ni peak signifies the progress of layer inversion.

Raman spectroscopy was used to check the phase formation of the samples, and the results are shown in Fig. 5. NiSi formation was confirmed at 600°C for all the Ni silicided poly-Si samples with and without ion implantation. At 700°C, no NiSi Raman peak was detected for all the samples at various sample locations. This shows

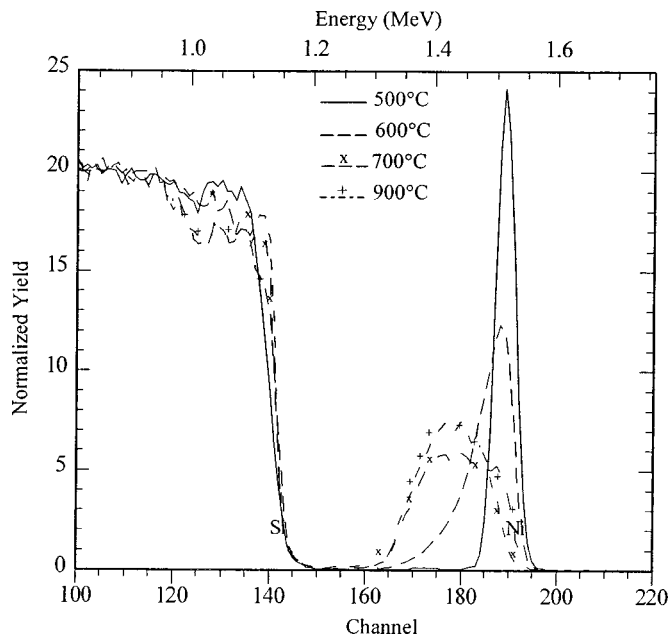


Figure 2. RBS analysis of Ni on poly-Si after annealing at 500, 600, 700, and 800°C.

that NiSi₂ has nucleated at 700°C on the poly-Si samples with and without ion implantation as suggested by the composition yield ratio of Ni to Si close to 1:2 at 700°C as shown in Fig. 2 to 4. From the Raman spectra obtained at 700°C on the undoped poly-Si, the huge peak at 302 cm⁻¹ belongs to the TA phonon Si and was attributed to the denuded Si regions due to extensive layer inversion.⁶ In contrast, the Raman spectra obtained from BF₂⁺ or N₂⁺ implanted poly-Si samples do not exhibit the 302 cm⁻¹ Si Raman peak, and the spectra resemble that of NiSi₂ on Si(100).⁷ This further confirms that layer inversion is less extensive on the implanted samples and that NiSi₂ has nucleated at 700°C.

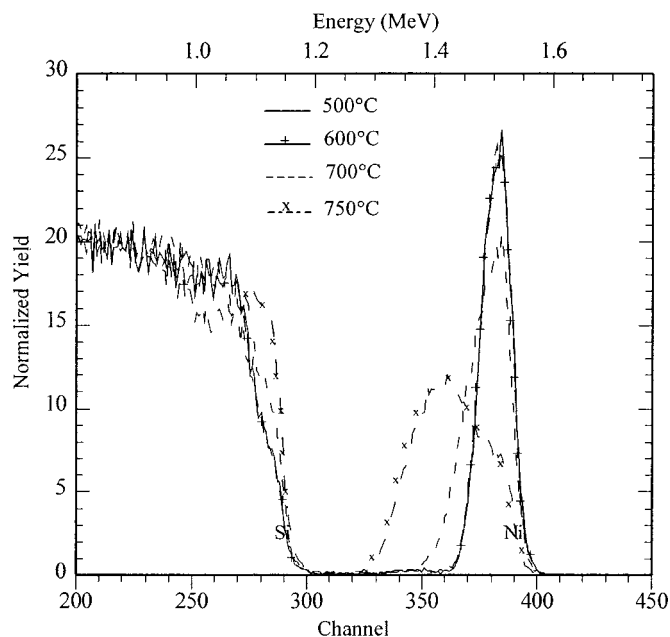


Figure 3. RBS analysis of Ni on BF₂⁺ implanted poly-Si after annealing at 500, 600, 700, and 750°C.

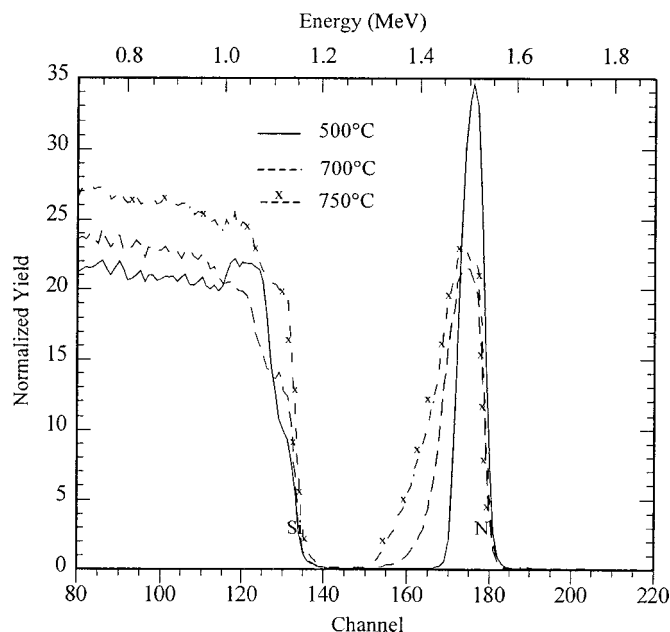


Figure 4. RBS analysis of Ni on N_2^+ implanted poly-Si after annealing at 500, 700, and 750°C.

The extent of layer inversion was further compared using the SEM analysis as shown in Fig. 6a to c. After annealing at 600°C, random exposure of holes in the silicide film is observed, and this is attributed to the extension of poly-Si toward the surface. It is obvious that improved morphology was achieved with the BF_2^+ and N_2^+ implanted poly-Si samples compared to the undoped poly-Si.

The sheet resistance behavior of Ni on the undoped and doped poly-Si is shown in Fig. 7. For samples with ion implantation and postimplant annealing, the change in sheet resistance is relatively small at 500 and 600°C compared to that on undoped poly-Si. At 700°C, a drastic increase is observed on the undoped poly-Si due to layer inversion. In contrast, the implanted samples have relatively

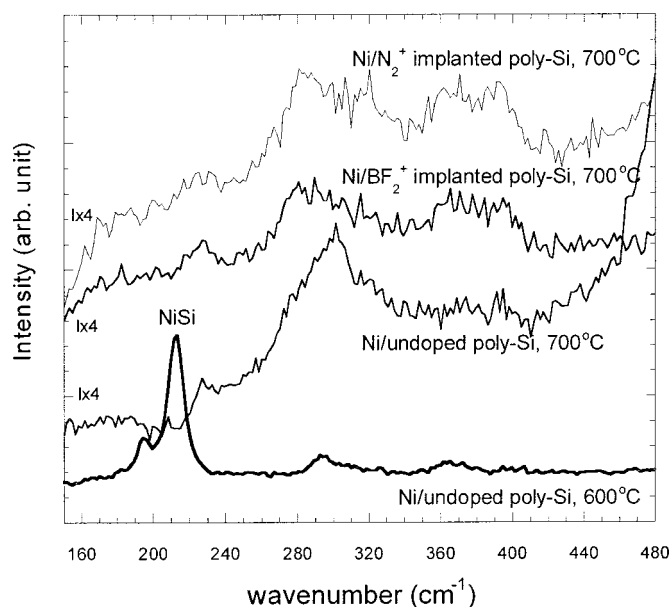


Figure 5. Raman analysis of Ni on undoped poly-Si after annealing at 600 and 700°C compared to Ni on BF_2^+ and N_2^+ implanted poly-Si after annealing at 700°C.

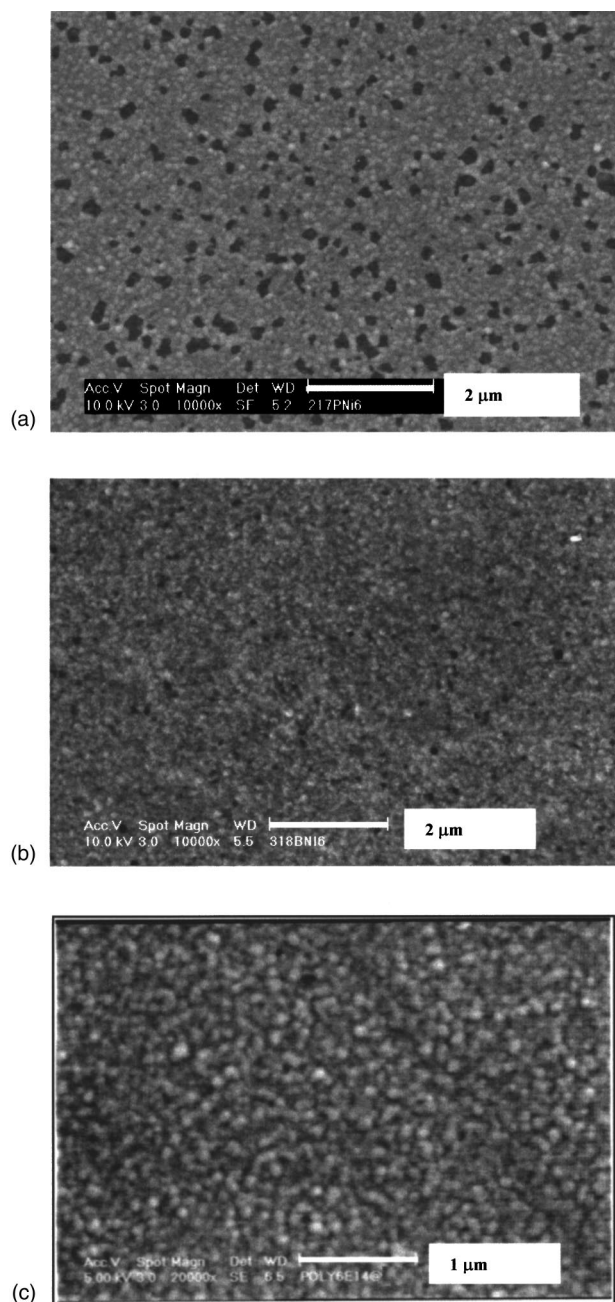


Figure 6. SEM analysis of Ni on (a) undoped poly-Si, (b) BF_2^+ implanted poly-Si, and (c) N_2^+ implanted poly-Si after annealing at 600°C.

stable sheet resistance. The rise in sheet resistance at 700°C can be attributed to both layer inversion and $NiSi_2$ nucleation. At 750°C, the sheet resistance increases to higher values in all cases due to the progression of layer inversion.

Discussion

It has been rationalized that there should not be a change in the thermodynamic driving force for the silicide-phase transformation on the poly-Si since the Si grain boundary energy is about one order of magnitude smaller than the difference in the heat of formation of $NiSi$ and $NiSi_2$, and two orders of magnitude smaller than the heat of formation of a typical silicide.⁸ We have previously found that $NiSi_2$ was formed with Ni silicidation on undoped poly-Si after annealing at 700°C.⁹ The slightly early nucleation of $NiSi_2$ on poly-Si compared to that on Si(100) at 750°C was attributed to the

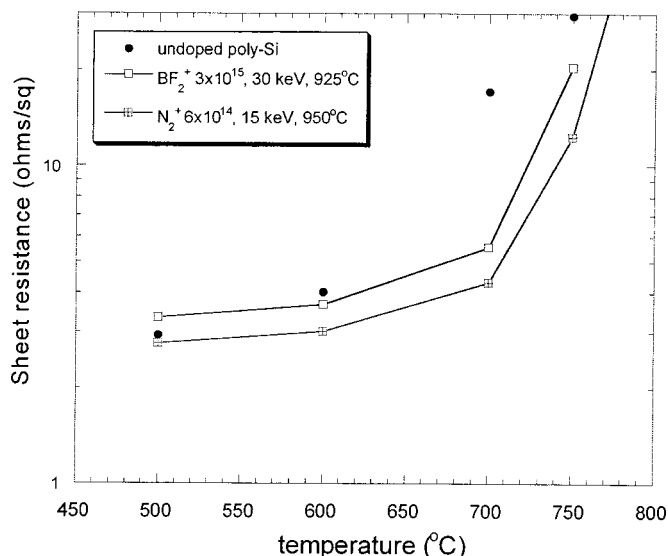


Figure 7. Sheet resistance of Ni on undoped poly-Si, BF₂⁺ implanted poly-Si, and N₂⁺ implanted poly-Si after annealing at various temperatures.

generation of a higher number of nucleation sites and/or a higher chance for the nuclei to be stabilized during the layer reconstruction. On the other hand, the compressive stress generated during NiSi₂ formation could be compensated by the tensile stress generation during layer inversion and lower nucleation barrier of NiSi₂. In this study, NiSi₂ was found to form on the poly-Si substrates with and without ion implantation (BF₂⁺ or N₂⁺) after annealing at 700°C. Therefore, NiSi₂ nucleation on poly-Si (whether doped or undoped) is more favorable compared to that on Si(100) or Si(111). The result is intriguing since layer inversion of the ion-implanted poly-Si samples was obviously suppressed at 600°C. The formation of NiSi₂ at 700°C therefore implies that layer inversion could have been initiated substantially at 700°C and consequently promotes the nucleation of NiSi₂.

The silicide-enhanced grain growth in poly-Si occurs mainly by the growth of existing grains via secondary grain growth. This can be driven solely by the reduction of the total energy associated with the normal grain boundaries. Differences in surface energy can supply an additional driving force for the growth of secondary grains. According to the secondary grain growth model,¹⁰ the driving force can be represented by

$$\Delta F = -\frac{2(\Delta\gamma)}{h} - \frac{1.15\gamma_{gb}}{r_n} + \frac{2\gamma_{gb}}{r_s}$$

where $\Delta\gamma$ is the surface energy anisotropy ($\Delta\gamma \equiv \bar{\gamma} - \gamma_{min}$), h the thickness, γ_{gb} the grain boundary energy, r_s the secondary grain size, and r_n the dimension of the normal grain matrix.

The initial as-deposited poly-Si comprises needle-like columnar grains that result in large $\Delta\gamma$ and γ_{gb} and thus have a high driving force for secondary grain growth. The Si for grain growth is provided by the small poly-Si grains at the bottom interface, which are consumed by the silicide until all the small poly-Si grains at the lower interface are consumed.¹¹ The poly-Si growth invades the silicide layer and ends up with much larger grains settling at the oxide interface.

Grain growth is a strong function of the diffusion coefficient of Si. Dopants in Si strongly influence the self-diffusion due to both electrical and dopant-point defect interaction effects. The dopant solubility in the grains and hence the dopant segregation (in cases where dopant concentration are extremely high) in the grain boundaries could influence the grain growth process. No dopant segregation was observed in B-doped poly-Si films.¹² It was reported that B

enhanced the grain growth of Si,¹³ but the effect of B on enhancing grain growth was observed to be fairly small.¹⁴ Since the BF₂⁺ implanted poly-Si has been shown to reduce layer inversion, the enhanced Si grain growth (compared to the undoped poly-Si case) prior to silicidation has contributed to the improved morphology by reducing the driving force for layer inversion.

On the other hand, it was expected that N would inhibit grain growth,^{15,16} since N (like C and O) is electrically inactive and possibly does not interact with point defects. In view of the low solubility of N in Si (around 5×10^{15} atom/cm³), the N atoms are likely to segregate at the grain boundaries of poly-Si changing the surface and/or grain boundary energy of the system and thus the grain growth. The effect of N on the inversion seems to be at least partially due to an inhibition of the poly-Si grain growth. Another effect of N on grain growth may be the formation of precipitates of Si nitride in the poly-Si. As the grain boundaries must move past the precipitate during Si grain growth, this is expected to limit the poly-Si grain growth.¹⁷ The dynamic dissociation/formation of silicides along the grain boundaries, which was proposed to be a process of silicide-enhanced layer inversion,¹⁸ would be affected.

The dopant distribution depth for BF₂⁺ 3×10^{15} , 15 keV without driving in was projected at about 30 nm (secondary ion mass spectroscopy and TRIM) and thus is within the Si consumption range for 30 nm of Ni during silicidation. The dopants incorporated in the silicide overlayer after silicidation may exert an effect in reducing layer inversion. A similar finding was obtained for agglomeration retardation in NiSi₂ in the presence of B and/or F atoms at grain boundaries.¹⁹ Similarly, the silicide grain boundary migration may be hindered by the presence of B or F atoms and was conjectured to prevent/delay the silicide dissociation, which leads to layer inversion. Since N is incorporated into the silicide layer after silicidation, the interfacial energy of silicide/poly-Si may be changed and affect the poly-Si grain growth process.

In addition, implantation usually introduces additional defects besides the large amount of defects like twin or stacking faults that exist in the poly-Si due to the low pressure chemical vapor deposition growth. The postimplant anneal may have removed most of the implantation damages. This is supported by a previous study where it was reported that on N-implanted Si(100), after a postimplant anneal at 900°C, there are fewer fine structure defects with a small density of rod defects and dislocation loops.²⁰ For the BF₂⁺ implant, solid-phase epitaxial recovery of the implantation-induced amorphous layer progresses at about 550°C on Si(100).²¹ This eliminates the high-energy state of the as-deposited or as-implanted poly-Si, and the stabilized poly-Si microstructures reduces the driving force for layer inversion.

Conclusions

We have shown that ion implantation using BF₂⁺ and N₂⁺ have suppressed layer inversion. The incorporation of dopants into the silicide layer can account for the change in the layer inversion behavior. In addition, the enhanced poly-Si grain growth due to BF₂⁺ implant was attributed to the reduced driving force for layer inversion. The inhibition of poly-Si grain growth by N ions has also been shown to be effective in suppressing layer inversion. The nucleation of NiSi₂ occurred at 700°C on the poly-Si samples with or without ion implantation, is attributed to a substantial initiation of layer inversion that has occurred at 700°C.

Acknowledgments

R. Lee and W. D. Wang are acknowledged for technical assistance. This work is supported in part by the NUS-CSM special project and an NSTB grant.

National University of Singapore assisted in meeting the publication costs of this article.

References

1. T. Morimoto, H. S. Momose, T. Inuma, I. Kunishima, K. Suguro, H. Okano, I. Katakabe, H. Nakajima, M. Tsuchiaki, M. Ono, Y. Katsumata, and H. Iwai, *Tech. Dig. Int. Electron Device Meet.*, **1991**, 653.
2. D.-X. Xu, S. R. Das, C. J. Peters, and L. E. Erickson, *Thin Solid Films*, **326**, 143 (1998).
3. T. Ohguro, M. Saito, T. Yoshitomi, T. Morimoto, H. S. Momose, Y. Katsumata, and H. Iwai, *IEEE Trans. Electron Devices*, **47**, 2208 (2000).
4. S. Nygren, D. Caffin, M. Ostling, and F. M. D'Heurle, *Appl. Surf. Sci.*, **53**, 87 (1991).
5. S. P. Murarka, *J. Vac. Sci. Technol. B*, **2**, 693 (1994).
6. P. S. Lee, D. Mangelinck, K. L. Pey, J. Ding, T. Osipowicz, C. S. Ho, L. Chan, G. L. Chen, *Mater. Res. Soc. Symp. Proc.*, **591**, 269 (2000).
7. P. S. Lee, D. Mangelinck, K. L. Pey, Z. X. Shen, J. Ding, T. Osipowicz, and A. See, *Electrochem. Solid-State Lett.*, **3**, 153 (2000).
8. E. Colgan, J. P. Gambino, and Q. Z. Hong, *Mater. Sci. Eng., R.*, **6**, 43 (1996).
9. P. S. Lee, D. Mangelinck, K. L. Pey, J. Ding, D. Z. Chi, J. Y. Dai, and A. See, *Microelectron. Eng.*, In press.
10. C. V. Thompson, *J. Appl. Phys.*, **58**, 764 (1985).
11. E. G. Colgan, J. P. Gambino, and B. Cunningham, *Mater. Chem. Phys.*, **46**, 209 (1996).
12. M. M. Mandurah, K. C. Sawasawt, C. R. Helms, and T. I. Kamins, *J. Appl. Phys.*, **51**, 5755 (1980).
13. T. Makino and H. Nakamura, *Solid-State Electron.*, **24**, 49 (1981).
14. L. Mei, M. Rivier, Y. Kwark, and R. W. Dutton, *J. Electrochem. Soc.*, **129**, 1791 (1982).
15. K. Nakazawa and T. Tanaka, *J. Appl. Phys.*, **68**, 1029 (1990).
16. G. L. Olson and J. A. Roth, *Mater. Sci. Rep.*, **3**, 1 (1988).
17. C. V. Thompson, *Annu. Rev. Mater. Sci.*, **20**, 245 (1990).
18. S. Nygren and S. Johansson, *J. Vac. Sci. Technol. A*, **8**, 3011 (1990).
19. W. J. Chen and L. J. Chen, *Appl. Phys. Lett.*, **70**, 2628 (1991).
20. H. J. Stein, *Mater. Res. Soc. Symp. Proc.*, **59**, 523 (1986).
21. M. Tamura, Y. Hiroshima, and A. Nishida, *Mater. Chem. Phys.*, **4**, 23 (1998).